www.gondwanags.org.in

Research Article

ISSN : 2455-1953

JGSR

Journal of Geosciences Research

Vol. 8, No.1, January, 2023, pp. 29-37

Geochemical Signatures of Platinum Group Elements in Ultramafic Rocks of Chotanagpur Gneissic Terrain, Eastern India and Their Genetic Control

Jugnu Prasad and Deepak Kumar Bhattacharya

University Department of Geology, Ranchi University, Ranchi-834008(JH), India.
(Corresponding author, E-mail: dkbprofru78@gmail.com)*

Abstract

Ultramafic rocks occur as intrusives in the form of lensoid bodies in the northwestern part of Chotanagpur Gneissic Terrain and consist mainly of olivine, orthopyroxene and clinopyroxene and are devoid of plagioclase. Based on distinct geochemical characteristics, the rocks have been identified as komatiites. The rocks are geochemically analogous to Al-undepleted Munro type (Al_2O_3/ TiO_2=17.88-54.73) with distinctly high MgO (26.2-35.62 wt%), Ni (958-1902 ppm) and Cr (21.32-3320 ppm) contents. These rocks are characterised by low CaO/Al_2O_3, (Gd/Yb)n, (La/Yb)n with positive Zr, Hf, Ti anomalies suggesting high degree partial melting of mantle under anhydrous conditions at shallow depth with garnet as a residual phase in the mantle restite. These high MgO volcanic rocks having elevated concentrations of Ni and Cr are potential hosts for Platinum Group Elements (PGE) owing to their primitive mantle origin and eruption at high temperatures. These rocks have low ΣPGE (29-269.02ppb) content with Ir (0.1-0.8ppb) and Ru (1.05-5.78ppb) among Iridium group PGE (IPGE); and Pt (5.04-18.72ppb), Pd(3.5-18.0ppb), Rh (0.22-0.84ppb) among Platinum group PGE (PPGE). The PGE abundances in komatiites were controlled by olivine fractionation. The Major, trace, REE and PGE composition of the rock suggest melting under anhydrous condition at shallow depth above the garnet stability field under S-undersaturated condition. Anhydrous melting associated with mantle plume activity gave rise to the rock which subsequently contaminated by lower crustal materials during magma ascent and emplacement.

Keywords: Chotanagpur Gneissic Terrain, Komatiite, Platinum Group Elements, Sulphur Undersaturation, Plume

Introduction

Platinum Group Elements (PGE: Pt, Pd, Rh, Ir, Os, Ru) show strong chalcophile and siderophile affinity and tradionally they are subdivided into two groups- the compatible IPGEs (Os, Ir, Ru) and the incompatible PPGEs (Rh,Pd,Pt; Fiorentini *et al*., 2011). The IPGEs often have a refractory characters and are mainly associated with spinel where as PPGEs tend to concentrate in base metal sulphides. PGE compositions in mantle-derived ultramafic-mafic magmas are considered as sensitive indicators to understand their petrogenetic evolution and sulphide saturation history. The behavior of PGEs and their abundance is controlled by several factors like mantle heterogeneity, enrichment-depletion, processes of the mantle, partial mantle melting, melt percolation, sulphide segregation and crystal fractionation (Mondal, 2011 and references therein). Higher concentration of PGE in ultramafic rocks in comparison to other rock types not only suggest their economic significance but their lower concentration are also useful as geochemical tools to evaluate chemical evolution of mantle through time and their role in crust forming processes (Condie and Kroner, 2013). The appearance of Platinum Group of Minerals (PGMs) is rare phenomena and usually develops due to high abundance of PGE concentration and favorable sulfur fugacity condition in the magma (Maier, 2005). The PGMs usually occur as disseminated grains in ultramafics and are mainly associated with either sulphides of Ni or Cu or in intergranular spaces between olivine and pyroxene. PGE abundances in mantle derived rocks especially komatiites have been documented by various workers. These rocks reflect degree of partial melting of hot and dry peridotite, sulphur saturation history, rate of ascent, degree of differentiation and contamination prior to eruption which in turn suggest their ability to extract compatible elements and thereby provide information on PGE abundances of mantle (Fiorentini *et al*., 2011; Said *et al*., 2011; Zhou *et al*., 2014; Balaram *et al*., 2013; Tushipokla and Jayananda, 2013; Manikyamba and Saha, 2014; Saha *et al*., 2015; Guo *et al*., 2020; Dora *et al*., 2022).

Worldwide occurrences of PGE are very limited and confined to plutonic or hypabyssal magmatic intrusions of Archaean-Palaeoproterozoic age. In India three old cratonic blocks *viz* Dharwar in southern India, Singhbhum in Eastern India and Bundelkhand in central India are the Archean terrain where plutonic to hypabyssal ultramafic intrusions of Archaean as well as early Proterzoic age are present. There are three well documented chromite bearing PGE prospects are reported in association with ultramafic complex at (a) Baula Nausahi in Odisha (b) Sittampundi anorthosite complex in Tamil Nadu and (c) Channagiri and Hanumalapura in Karnataka. Recent studies show that there is

(Received : 04 April 2022 ; Revised Form Accepted : 28 September 2022)

https://doi.org/10.56153/g19088-022-0102-22

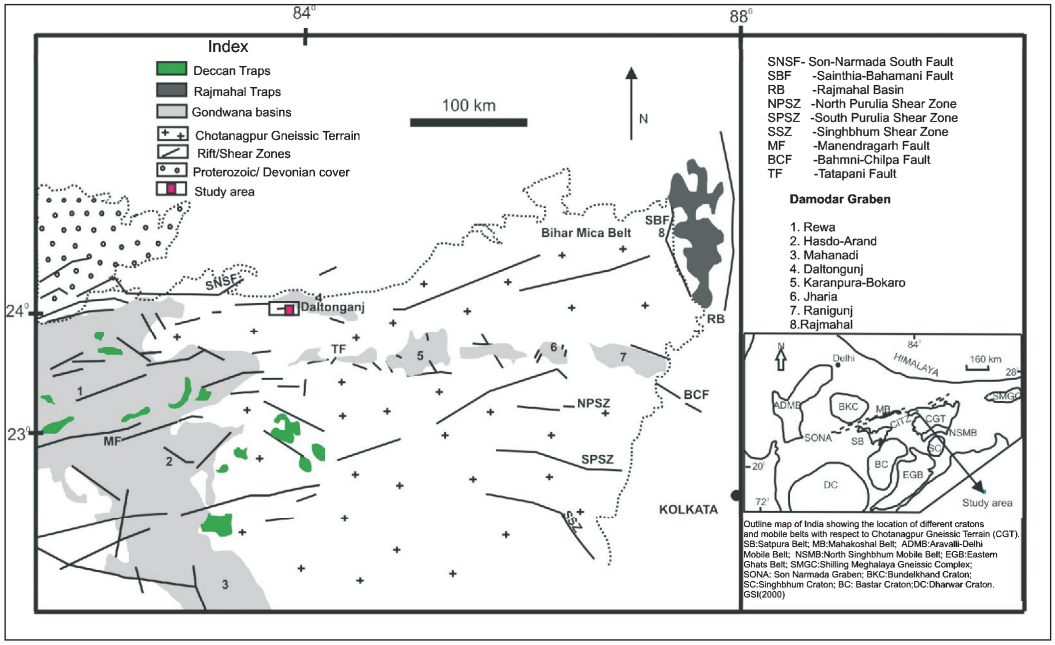

Fig. 1. Geological map showing various tectonic elements in the Chotanagpur Gneissic Terrain (*Modified after*, Rao *et al.*, 2014)

tremendous potential for PGE in mafic-ultramafic and ophiolite complexes occurring in different parts of India.

A number of mafic-ultramafic dykes/sills intrude the basement rocks of Chotanagpur Gneissic Terrain (CGT). In the northwestern part of CGT near Semra village (N23° 59'59": E83° 58'44"), 17 kms southwest of Medninagar town (formely known as Daltonganj town) and adjacent to Gondwana graben, the PGE and associated PGM in the ultramafic rocks of komatiitic composition have been recorded for the first time . A preliminary information on geochemical nature of PGEs content in these rocks has been discussed by Prasad and Bhattacharya (2013). In the present work we reassess major, trace, REE and PGE signatures of these ultramafic rocks to evaluate source characteristic, mantle melting conditions and sulphide saturation history on the basis of newly generated geochemical data.

Geological Setup

A roughly WNW-ESE trending orogenic belt called Central Indian Tectonic Zone (CITZ) dissects the Indian Shield into two halves and represents a major paleosuture along which different Archaean and Palaeoproterozoic blocks of Indian Shield are believed to have fused to form the "Greater Indian Landmass" (Bhowmik, 2019; Negi *et al*., 2022). The CGT which is a vast tract in the Peninsular Eastern Indian Shield represents the eastern extension of CITZ and comprises of gneisses and migmatites with patches of supracrustals composed of metamorphosed pelites, calcareous and psammitic sediments. Younger mafic, ultramafic and alkaline intrusive are also present. Number of mafic dykes have been studied highlighting the importance of igneous and tectonic processes in CGT (Prasad *et al*., 2012; Patel *et al*., 2021). Suites of peridotitic komatiite from Palamau district of Jharkhand (Bhattacharya *et al*., 2010) indicate that the mantle activities have occurred in the terrain. The ultramafic and mafic rocks of unknown geochemical affinity that emplaced at 1925±110 are suggested to be the oldest magmatic units (Rekha *et al*., 2011) in CGT.

The rocks of CGT display varying degrees of metamorphism and tectonic deformation occurring at ~2.5, 1.6-2.5, 1.2-1.0 and 0.9 Ga (Sanyal and Sengupta, 2012). Based on published geological and geochronological information a three fold subdivision of CGT is proposed extending from south to north (Mukherjee *et al*., 2019). The three domains designated as I, II and III are characterized by their gross lithology, metamorphism and deformational history. However, most of the ages reported from CGT are from the metamorphosed basement lithology. Thus the evolutionary history of CGT has remained speculative due to lack of sufficient geological information from the magmatic rocks. Ghose and Chatterjee (2008) recognized five major intra continental rift/ shear zones that control magmatism in CGT. Four of them namely South Purulia Shear Zone (SPSZ), North Purulia Shear Zone (NPSZ), Damodar Graben and South Narmada South Fault (SNSF) located from south to north of CGT trending ENE-WSW to E-W. The fifth runs N-S coinciding with Rajmahal Basin. The present area of investigation lies adjacent to Damodar-Graben (Fig. 1) suggesting emplacement of the studied ultramafic bodies in an extensional tectonic regime.

Analytical Techniques

Major oxides of ten number of representative samples selected on the basis of petrographic study were analysed by XRF at National Geophysical Research Institute (NGRI), Hyderabad (India). A Phillips Magi X PROPW2440 fully automatic, microprocessor controlled, 168-position automatic PW 2540 with VRC sample changer Wavelength dispersive X-ray Spectrometer was used for the determination of major oxides. International geochemical standard reference material from Geological Survey of Japan (JB-2, Basalt) was used to prepare calibration curves for major elements (Krishna *et al.*, 2007). From the analyzed value of JB-2, the error limits of measurement for major elements are within 5%. Trace and rare elements were analysed at NGRI, Hyderabad using Inductively Coupled Plasma Mass Spectrometer (ICP-MS),

model Perkin Elmer SCIEX EIAN DRC-II. The analytical procedure, calibration and standard followed are followed *after* Govindaraju (1994). To ensure precision of data, International Standard UB-N (serpentine) was used for calibrating the instrument and closed vessel digestion method has been employed for the analysis. PGE concentrations were estimated by using nickel Sulphide Fire- assay pre-concentration with Te-Co precipitation method followed by Inductively Coupled Plasma Mass Spectrometry (ICP-MS; Perkin Elmer Ellan DRC-II). Reference material WMG-1(Mineralised Gabbro) was utilized for calibrating the instrument and to monitor the accuracy of the data. Au and PGE were analysed following the process suggested by Balaram (2008). The detection limits of most of the elements including PGE were about 0.01mg/ml, and the precision is better than 6% for trace and REE, and is <10% for PGE analysis.

Petrographic Characteristics

The ultramafic rocks are dark grey medium to coarse grained massive and composed mainly of olivine and pyroxene. The primary igneous mineralogy has been altered to serpentine-termolite-actinolite-chlorite-talc-magnetite assemblage. Spinifex zone of this rock exhibits random and platy spinifex textures defined by criss-cross arrangement of primary minerals like olivine and pyroxenes (Fig. 2a). Olivine crystals are altered to serpentine and secondary magnetite whereas pyroxene plates are mostly altered to tremolite. The essential minerals of the cumulate zone are olivine pseudomorphosed by serpentine and magnetite, clinopyroxene and tremolite. These are usually olivine ortho to adcumulates (Fig. 2b) with decreasing amount of intercumulates material towards the base of the flow. Intercumulus phases are mainly pyroxene with fine grained magnetite, Cr-spinel, serpentine and talc. Cumulus olivine grains are dominantly subhedral and equant to tabular. The rock is characterized by complete absence of plagioclase. The large observed variation of LOI content is due to the variable proportions of secondary phases such as serpentine, tremolite, chlorite and talc which attest that the rock have been suffered metamorphism up to greenschist to lower amphibolites facies.

The signature of sulphur enrichment in these rocks is marked by appearance of dark color sulphide phases and sometimes by leaching of light yellow colored minerals on the weathered surface. The granular aggregates of PGE bearing minerals and sulphide of nickel and copper are present in the interstitial spaces of cumulates of olivine and pyroxenes.

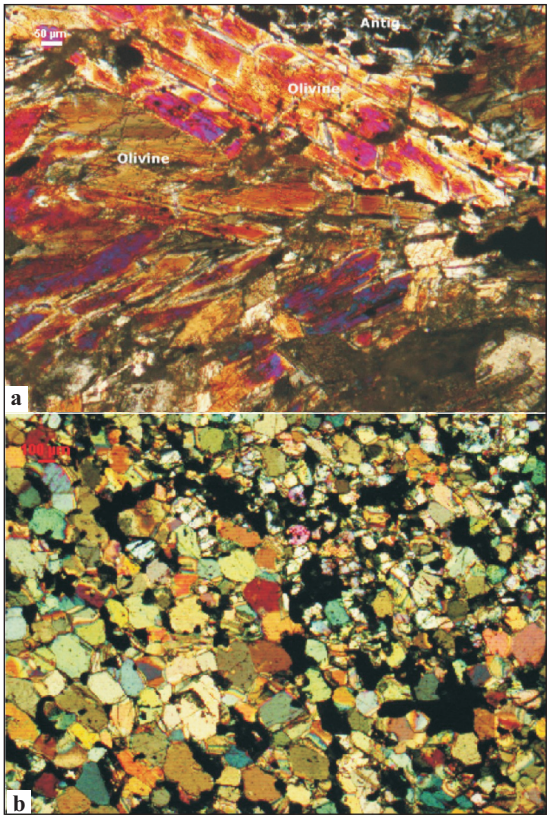

Fig. 2 a. Photomicrograph showing platy spinifex texture exhibited by criss-cross arrangement of olivine crystals. b. Photomicrograph showing anhedral to subhedral olivine grains randomly oriented making ortho to adcumulates texture

Results

The results of major oxides, trace elements, REE and PGE analyses of the studied rocks are presented along with analyses of some typical occurrences of the world (Table 1-4).

Table 1: Major oxide (in wt%) analysis of the ultramafic rocks of the study area along with some typical occurrences of the world

Sample no	PD5	PD11	PD8	PD4	PD3	PD1	PD21	PD6	PD7	PD9	BGB	AGB	GI	WDC	PM
SiO_2	35.6	36.01	40.23	43.01	39.62	40.66	41.45	36.92	37.01	38.16	47.2	45.1	43.48	45.67	45
TiO_2	0.2	0.21	0.19	0.22	0.22	0.23	0.41	0.11	0.18	0.22	0.3	0.31	0.49	0.73	0.2
Al_2O_3	5.58	5.22	6.63	7.8	6.57	6.88	7.01	6.02	6.53	6.8	3.4	6.3	9.6	12.61	3.65
Fe_2O_3	9.92	9.68	11.22	10.52	11.02	12.5	12.66	10.08	10.58	10.51		11.4	11.2	9.01	
MnO	0.31	0.12	0.1	0.12	0.15	0.14	0.14	0.22	0.24	0.22	0.2	0.15	0.17	0.11	0.13
MgO	35.62	34.52	31.11	26.2	31.76	30.02	29.15	34.22	33.02	32.88	31.4	30	21.9	21.97	37.8
CaO	5.44	5.61	6.02	6.88	5.98	5.08	5.01	6.52	6.48	6.16	5.6	5.7	8.6	4.18	3.55
Na_2O	0.31	0.33	0.28	0.31	0.38	0.07	0.15	0.14	0.27	0.23	0.07	0.34	0.64	0.08	0.33
K_2O	0.23	0.27	0.22	0.31	0.02	0.22	0.25	0.37	0.13	0.14	0.04	0.05	0.04	0.05	
P_2O_5	0.03	0.02	0.02	0.03	0.01	0.01	0.02	0.03	0.05	0.02	0.02	0.01	0.04	0.06	
LOI	6.68	7.88	5.01	5.22	5.02	5.21	5.24	4.98	4.21	4.58		7.5	5.3	5.39	
Total	99.74	99.87	101.03	100.62	100.75	101.02	101.79	99.61	100.89	99.9					
Mg#	88.03	87.75	84.61	83.33	84.95	83.14	82.75	87.62	85.05	86.31					
Al_2O3/TiO_2	27.9	24.86	34.89	35.45	29.86	29.91	17.88	54.73	34.61	34					
CaO/Al_2O_3	0.97	1.07	0.91	0.88	0.91	0.78	0.71	1.08	0.99	0.9					
CaO/TiO_2	27.2	26.71	31.68	31.27	27.18	22.09	12.21	59.27	36	28					
MgO/TiO_2	178.1	164.4	163.73	119.09	144.36	130.52	71.1	311.09	183.44	149.45					
MgO/Al_2O_3	6.38	6.61	4.69	3.36	4.83	4.36	4.18	5.68	5.05	4.84					

Table 2: Trace elements(in ppm) analysis of the ultramafic rocks of the study area along with some typical occurrences of the world

Sample no	PD5	PD11	PD8	PD4	PD3	PD1	PD21	PD6	PD7	PD9	BGB	AGB	GI	WDC	PM
Ni	1902	1881	1138	958	1208	1057	1025	1709	1507	1452	1611	1633	997	834.87	1960
Cu	85	81	51	35	66	42	37	78	72	71					30
Co	95	91	60	52	66	63	57	78	71	69					
Cr	3320	3008	2532	2132	2608	2350	2223	2908	2892	2690	2910	2600	2323	2246	2625
Rb	0.49	0.52	0.76	0.81	0.68	0.77	0.83	0.59	0.63	0.63					0.6
Sr	9	11	15	18	14	19	17	11	12	12					19.9
Cs	0.02	0.03	0.04	0.04	0.03	0.05	0.04	0.05	0.04	0.03					0.02
Zn	47	51	44	65	32	55	68	46	40	38					55
Sc	19.2	17.6	25.8	31.2	24.2	33.3	37.7	18.8	22	23.8				17.37	16.2
V	52	82	127	168	108	143	152	76	83	92				153.5	82
Nb	0.11	0.13	0.36	0.88	0.33	0.52	0.82	0.05	0.18	0.27	1.05	0.4	0.6	0.92	0.66
Ta	0.6	0.58	0.22	0.28	0.17	0.19	0.22	0.06	0.09	0.09				0.04	0.04
Zr	12	15	33	35	27	36	38	18	21	29	19.1	15	19.2	58.5	10.5
Hf	0.09	0.12	0.37	0.42	0.29	0.4	0.4	0.22	0.22	0.28				1.32	0.28
Y	7.51	7.23	10.81	15	10.9	11.5	13	8.02	8.18	9.52	6.8	7.6	12.3	12	4.3
Ti	1199	1259	1139	1319	1319	1379	2458	659	1079	1319					1205
U	0.02	0.08	0.07	0.44	0.02	0.08	0.03	0.02	0.02	0.08				0.24	0.02
Th	0.02	0.09	0.06	0.45	0.03	0.09	0.02	0.03	0.06	0.09	0.1	0.04	<0.5	0.49	0.08
Ratios															
Ti/Zr	99.91	83.93	34.51	37.68	48.85	38.3	64.68	36.61	51.38	45.48					
Ti/Y	159.7	174.1	105.36	87.93	121	119.91	189.07	82.16	131.9	138.55					
Ti/Sc	62.44	71.53	44.14	42.27	54.5	41.41	65.19	35.05	49.04	55.42					74.38
Ti/V	23.05	15.35	8.96	7.85	12.21	9.64	16.17	8.67	13	14.33					14.69
Zr/Y	1.59	2.07	3.05	2.33	2.47	3.13	2.92	2.24	2.56	3.04					2.44
Zr/Sc	0.62	0.85	1.27	1.12	1.11	1.08	1	0.95	0.95	1.21					0.65
Sc/Y	2.55	2.43	2.38	2.08	2.22	2.89	2.9	2.34	2.68	2.5					
V/Zr	4.33	5.46	3.84	4.8	4	3.97	4	4.2	3.95	3.17					
V/Sc	2.7	4.65	4.92	5.38	4.46	4.29	4.03	4.04	3.77	3.86					5.06
Ni/Cu	22.37	23.22	22.31	27.37	18.3	25.16	27.7	21.91	20.93	20.45					
Nb/Y	0.01	0.02	0.03	0.06	0.03	0.06	0.06	0.01	0.02	0.03					

The rocks of the area are characterised by low SiO_2 (35.6-43.01), CaO (5.01-6.88), TiO_2 (0.11-0.23) Na_2O (0.07-0.38), K_2O (0.02-0.27), moderate Al_2O_3 (5.22-7.8), Fe_2O_3 (9.68-12.66), high MgO (26.2-35.62) and Loss on ignition (LOI) varies from 4.21 to7.88. Al_2O_3- (Fe_2O_3 + TiO_2)- MgO (Jenson, 1976; Viljoen *et al*., 1982; Fig. 3a) and CaO- MgO- Al_2O_3 diagrams (Viljoen *et al*., 1982; Fig. 3b) classify these ultramafic rocks as komatiite which is consistent with their major oxide compositions. Al_2O_3/TiO_2 (17.88-54.73) and CaO/Al_2O_3 (0.71-1.08) ratios suggest that the komatiites of the area are geochemically analogous to Al-undepleted Munro type komatiites. Al_2O_3, SiO_2, Fe_2O_3, TiO_2 and CaO exhibit negative correlation with MgO (Fig.4a).

The rocks are characterized by high concentrations of compatible trace elements like Ni (958-1902 ppm), Co (52-95 ppm) and Cr (2132-3320 ppm) with relatively lower concentrations of incompatible large ion lithophile elements (LILE) such as Rb (0.49-

Table 3: Rare Earth Elements (in ppm) analysis of the ultramafic rocks of the study area alongwith some typical occurrences of the world

Sample no	PD5	PD11	PD8	PD4	PD3	PD1	PD21	PD6	PD7	PD9	BGB	AGB	GI	WDC	PM
La	0.29	0.46	0.69	0.88	0.66	0.76	0.87	0.56	0.81	0.72	1.2	0.4	0.8	3.25	0.65
Ce	0.87	0.91	1.69	2.31	2	1.93	2.24	0.98	1.44	1.56	3.2	1.3	2.1	9.23	1.6
Pr	0.09	0.17	0.36	0.85	0.17	0.2	0.18	0.1	0.2	0.37				1.33	0.25
Nd	0.51	0.54	1.09	1.81	1.52	1.67	0.81	0.62	0.98	1.31	2.5	1.4	2.1	6.09	1.25
Sm	0.12	0.2	0.41	0.79	0.19	0.43	0.28	0.26	0.28	0.4	0.8	0.6	0.9	1.82	0.41
Eu	0.09	0.09	0.42	0.88	0.42	0.56	0.61	0.11	0.18	0.22	0.3	0.2	0.4	0.53	0.15
Gd	0.56	0.62	0.86	1.15	0.82	0.95	0.88	0.73	0.67	0.57	0.9	0.9	1.5	2.33	0.54
Tb	0.08	0.09	0.15	0.21	0.14	0.17	0.16	0.11	0.11	0.14				0.43	0.09
Dy	18	0.2	0.41	1.32	0.35	0.44	1.03	0.27	0.32	0.32	1.08	1.2	2	2.44	0.67
Ho	0.04	0.06	0.21	0.41	0.18	0.27	0.33	0.09	0.11	0.13				0.5	
Er	0.18	0.21	0.67	0.98	0.44	0.72	0.77	0.29	0.38	0.43	0.6	0.8	1.3	1.36	0.44
Tm	0.05	0.08	0.14	0.21	0.13	0.15	0.17	0.11	0.17	0.14				0.21	0.07
Yb	0.68	0.68	1.11	1.33	1.02	1.1	1.12	0.88	0.64	0.66	0.6	0.8	1.3	1.32	0.44
Lu	0.04	0.06	0.17	0.21	0.15	0.18	0.22	0.09	0.12	0.1				0.19	
(La/Nb)n	2.65	3.74	1.93	1.02	2.04	1.48	1.07	10.75	4.63	2.71					
(La/Ta)n	0.03	0.05	0.18	0.18	0.22	0.23	0.23	0.53	0.52	0.46					
(La/Sm)n	0.17	0.16	0.12	0.08	0.25	0.12	0.22	0.15	0.21	0.13					
(Gd/Yb)n	0.66	0.74	0.63	0.71	0.66	0.7	0.64	0.68	0.86	0.71					
(La/Yb)n	0.34	0.46	0.43	0.46	0.44	0.48	0.59	0.44	0.87	0.75					
(Sm/Nd)n	0.24	0.37	0.37	0.44	0.12	0.26	0.35	0.42	0.29	0.31					
(Th/Nb)n	1.49	5.7	1.38	4.3	0.76	1.44	0.2	4.75	2.81	2.78					
(Sm/Yb)n	1.69	2.82	3.53	5.68	1.79	3.75	2.39	2.84	4.2	5.79					
La/Nb	2.63	3.53	1.91	1	2	1.46	1.06	11.2	4.5	2.66					
La/Ta	0.48	0.79	3.13	3.14	3.88	4	3.95	9.33	9	8					
La/Sm	2.14	2.3	1.68	1.11	3.47	1.76	3.1	2.15	2.89	1.8					

Table 4: Platinum Group Elements(in ppb)analysis of the ultramafic rocks of the study area alongwith some typical occurrences of the world

Sample no	PD5	PD11	PD8	PD4	PD3	PD1	PD21	PD6	PD7	PD9	BGB	AGB	GI	Chrondrite	PM
Ru	5.78	4.61	1.47	1.05	4.22	1.08	1.29	3.69	3.05	2.88	4.3	5.31	3.3		5
Rh	0.44	0.42	0.78	0.57	0.22	0.71	0.68	0.84	0.81	0.81					0.9
Pd	18	15.55	4.22	4.2	12.01	3.8	3.5	12.78	8.76	6.61	5.51	10.6	12		3.9
Pt	16.62	18.72	6.64	5.23	13.12	6.62	5.04	11.15	9.29	7.13	5.83	11.1	14.1		7.1
Re	10.01	7.6	4.7	2.8	8.8	3	2.2	8.2	5.6	5.8					
Ir	0.8	0.75	0.3	0.1	0.5	0.3	0.11	0.5	0.4	0.1	1.23	2.13	2.05		3.2
Au	62.04	137	238.2	15.05	38.2	34.5	256.2	38.8	14.98	39.12					1
PGE+Au	113.7	184.7	256.31	29	77.07	50.01	269.02	75.96	42.89	62.45					
Cu/Pd	4.72	5.21	12.09	8.33	5.5	11.05	10.57	6.1	8.22	10.74					
Cu/Ir	106.3	108	170	350	132	140	336.36	156	180	710					
Pd/Ir	22.5	20.73	14.07	42	24.02	12.67	31.82	25.56	21.9	66.1				1	1
Pd/Ru														0.79	0.79
Pd/Rh														2.73	2.75
Pd/Pt	1.08	0.83	0.64	0.8	0.91	0.57	0.69	1.15	0.94	0.93				0.53	0.53
Pt/Pd	0.92	1.2	1.57	1.25	1.09	1.74	1.44	0.87	1.06	1.08					1.82
Ni/Pd	105.7	121	269.66	228.09	100.58	278.16	292.86	133.73	172.03	219.67					
Ru/Ir	7.23	6.15	4.9	10.5	8.44	3.6	11.73	7.38	7.63	28.8				1.28	1.27
Pt/Ir	20.78	24.96	22.13	52.3	26.24	22.066	45.82	22.3	23.22	71.3					
Total IPGE	6.58	5.36	1.77	1.15	4.72	1.38	1.4	4.19	3.45	2.98					
Total PPGE	97.1	171.7	249.84	25.05	63.55	45.63	265.42	63.57	33.84	53.67					
IPGE/PPGE	0.07	0.03	0.01	0.05	0.07	0.03	0.01	0.07	0.1	0.06				0.99	0.99
PPGE/IPGE	14.76	32.03	141.15	21.78	13.46	33.07	189.59	12.17	9.81	18.01				1.01	1.01

Present data: PD1 to PD21- ultramafic rocks of Semra, Palamau district, Jharkhand

BGB-Barberton Greenstone Belt (Smith and Erlank, 1982),

AGB(Abitibi Greenstone Belt)- Munro, Alexo, Pyke hill, Boston (Puchtel *et al.*, 2004), GI Gorgona Island Basaltic Volcamism Study Project, 1981, WDC-Western Dharwar Craton (Tushipokla and Jayananda, 2013), PM- Primitive mantle (McDonough and Sun, 1995) and Chondrite (Sun andMcDonough, 1989)

Mg#=100Mg/Mg+Fe^{+2}

0.83 ppm) and Sr (9-19 ppm). High field strength elements (HFSE) like Nb (0.05- 0.88 ppm),Ta (0.06-0.58) and Hf (0.09-0.4 ppm) show extremely depleted concentrations except Zr (12-38 ppm) that shows relatively higher range. Ni and Cr show positive correlation with MgO whereas HFSE like Zr, Nb, Yb, Sc, Ta as well as Y increase with decreasing MgO content (Fig. 4b). The rock shows wide range of Ni and Cu concentrations which is reflected in Ni/Cu ratios. The ratio of Zr/Y is less than 1 and that of primitive mantle value of 2.4. In the primitive mantle normalized multi-element patterns Nb shows negative whereas Ta, Zr, Hf and Ti exhibit positive anomalies (Fig. 5a). LHREEs are 2 to 3 times enriched than HREEs. Gd,Yb, La, Ce, Sm, Nd show increasing trends with decreasing MgO content (Fig. 4c). In the chrondrite normalized spider diagram (Fig. 5b) LREE is depleted to flat to slightly enriched HREE which is consistent with other such komatiites with high Al_2O_3/TiO_2 ratios (Blichert-Toft *et al*., 2015).

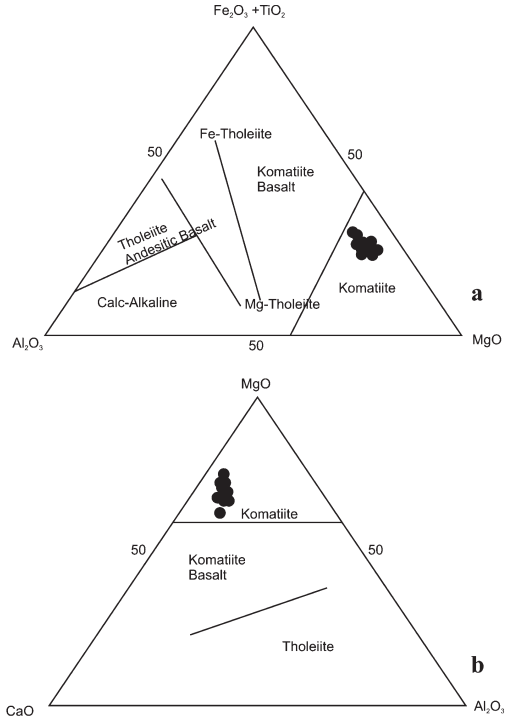

Fig. 3 a. Al_2O_3-(Fe_2O_3 + TiO_2)- MgO triangular plot(Jenson, 1976; *modified after*, Viljoen *et al.*, 1982), b. CaO-MgO-Al_2O_3 triangular plot (*after* Vilijoen *et al.*, 1982) showing the komatiitic nature of ultramafic rocks

The PGE contents of komatiites are low (<100 ppm) and total PGE ranges from 10.76 to 42.46 ppb with Ir 0.1 to 0.8 ppb, Ru 1.05-5.78 ppb) among IPGE and 5.04-18.72 ppb Pt, 3.5-18 ppb Pd and 0.22-0.84 ppb Rh among PPGE. Os was not taken into account as it is not possible to quantify Os by NiS fire assay method. Au ranges from 14.98 to 256.2 ppb. The concentration of Pd, Pt and Au are higher than the primitive mantle values of 3.9, 7.1 and 1.0 respectively for most samples whereas values of Ru, Ir and Rh are lower than the primitive mantle values (Table 4; McDonough and Sun, 1995).The rock type have Pd/Ir (12.67-66.1) and Pd/Pt (0.57-1.15) higher than the primitive mantle values (Pd/Ir-1.01, Pd/Pt-0.53; McDonough and Sun, 1995). Pt/Pd ratio in most of the samples is more than 1. In most samples Pd/Ir is more than Pt/Pd (Table 4). High ratio of Pt/Ir (20.77-71.3) and enrichment of Pd are attributed to fractional crystallization of parental magma. The Ni/Cu ratios of the rock is very similar to PGE mineralization associated with komatiite magmatism (Lesher and Barnes, 2009).The plots of Ni, Ir, Pt and Pd with MgO show a common positive trend. In the primitive mantle normalized diagram there is sharp anomaly of Pd, Pt and Au. The PGE contents of most of the samples are in the global range of Al-undepleted komatiites with up to 15.1 ppb Pt, 20.9 ppb Pd, 8.99 ppb Ir, 6.35 ppb Ru and 27.7 ppb. Au (Guo *et al*., 2020). Except for Ir the studied rocks exhibit near similarities with global range.

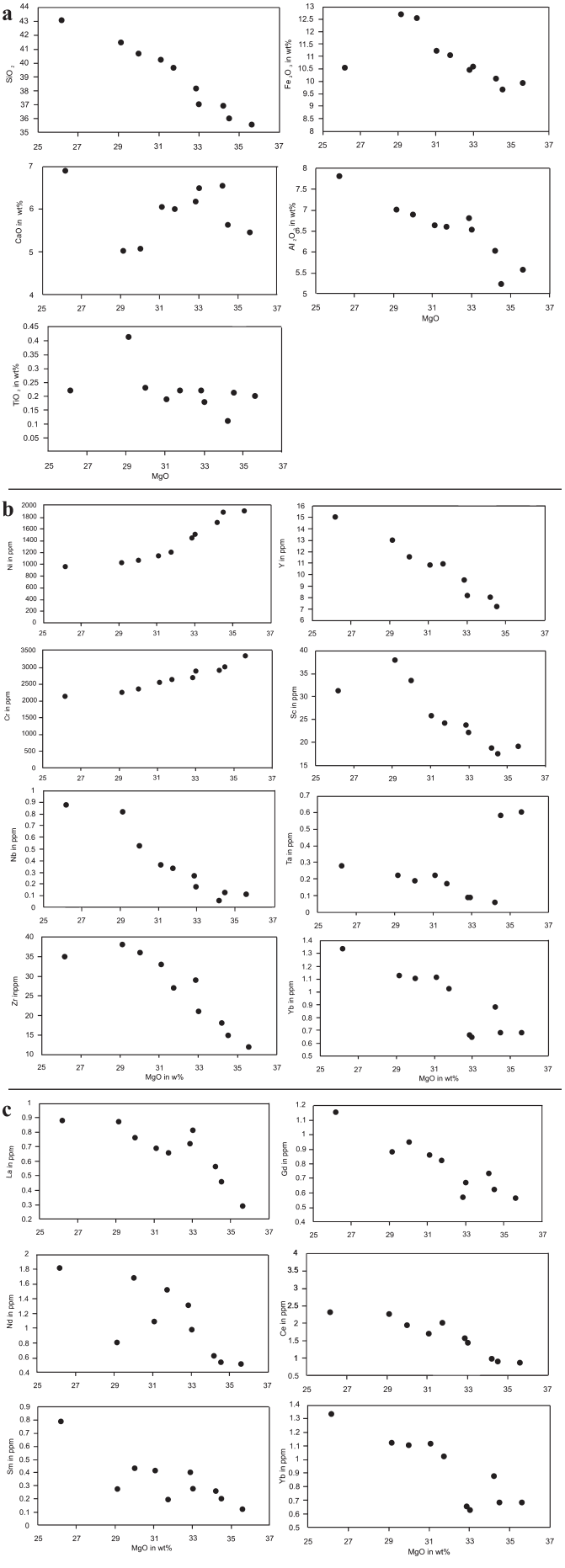

Fig. 4 a. Geochemical trend of major oxides showing the crystallization trend of ultramafics of the study area (Harker's binary diagram), b. MgO vs trace elements variation diagram for komatiites of the area, c. MgO *vs* different REEs variation diagram

Discussion

In the northwestern fringe of CGT, ultramafic rocks having mineralogically and chemically similar to komatiite, occur as lenses of varying dimension intercalated with metasedimentary rocks and follow the regional foliation trend (ENE-WSW) of the country rock . The various major oxides viz, Al_2O_3, SiO_2, TiO_2 and Fe_2O_3 exhibit negative correlation with MgO which point out a distinct and strong trend of crystallization of the rock caused by olivine accumulation and fractionation. Ni and Cr concentrations have been considered as very sensitive indicators of olivine, spinel and chromite crystallization from ultramafic magma (Maier *et al*., 2005; Lesher and Barnes, 2009; Naldrett, 2010). Ni and Cr show positive correlation with MgO which could be related to olivine

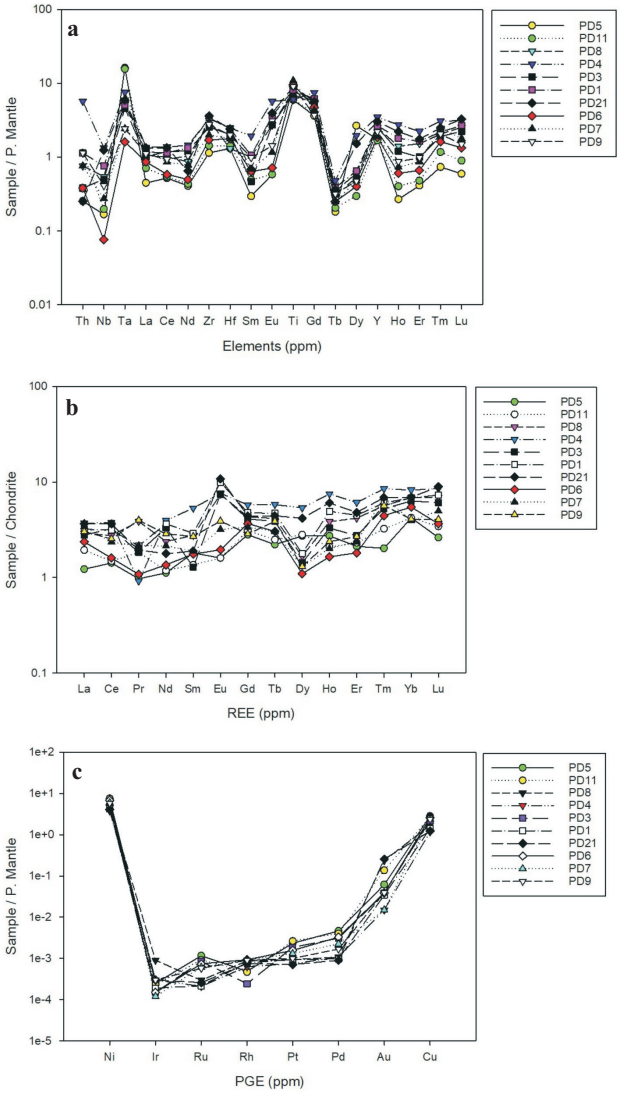

Fig. 5 a. Primitive mantle - normalized multielement variation diagram of the komatiites of the area (*after,* Sun and McDonough, 1989), b. Chrondrite-REE normalized spider diagram of komatiites of the area (*after* Sun and McDonough, 1989), c. Primitive mantle- normalized Platinum Group Element distribution pattern (McDonough and Sun 1995)

fractionation, HFSE like Zr, Nb, Yb, Ta as well as Y increase with decreasing MgO content consistent with them being incompatible in olivine. Co and Cu are incompatible in most of the silicates and oxide phases that crystallize from mafic-ultramafic magmas but strongly compatible in sulphides in komatiite. Cu abundances increase during fractionation and become concentrated in the magma during removal of other components in crystallizing phases. Co concentration in the rock increases with MgO and are consistent with accumulation of olivine. The abundances of Sc in komatiites are strongly determined by whether all of the garnet was consumed during melting or whether it remained as a residue phase in the residue. The rise in the abundance of Sc with the decreasing MgO content confirms that it is incompatible in olivine. Gd, Yb, La, Ce, Sm, Nd show decreasing values with increasing MgO content consistent with them being incompatible in olivine.

The plot (Gd/Yd)n vs Al_2O_3/ TiO_2 (Fig. 6), and ratios of Al_2O_3/ TiO_2, CaO/Al_2O_3, CaO/TiO_2 MgO/ TiO_2, MgO/Al_2O_3, (Gd/Yb)n, Nb/Y, La/Nb suggest that the rock of the area is geochemically analogous to Al-undepleted Munro type Komatiite, the most common variety of Mesoarchaean to Neoarchean komatiites globally (Dostal and Muellar, 2004).

Low $CaO/Al_2O_3$and (Gd/Yb)n and High Al_2O_3/TiO_2 HREE, Y and Zr suggest derivation of the rock from shallow upper mantle without garnet involvement (Maya *et al*., 2017). In the primitive mantle normalized spider diagram LREE is depleted to flat to slight enriched HREE which is consistent with other such komatiites with high Al_2O_3/ TiO_2 ratios (Blichert and Toft *et al*., 2015).Low abundance of incompatible lithophile elements (Ti, Nb, Ta, LREE) moderate Zr, Y, MREE, HREE and high abundance of compatible elements (Ni, Ca, Mg) all attest that these rocks are derived from high degree of partial melting of a long term depleted mantle source (Arndt *et al*., 2008) where Mg rich olivine and orthopyroxene were dominant phase entering the melts. Low large ion lithophile elements and Th/Yb ratio of the studied rocks are consistent with an undepleted mantle source .The undepleted nature of the komatiites are better explained by partial melting in rising mantle plume that originated at depths less than 200 Km where olivine is liquidus phase and magma is less dense than olivine. These rocks are subsequently modified by crustal contamination by lower crustal materials during magma ascent and emplacements. Crustal contamination plays a significant role in sulphur saturation history and brings about PGE mineralization (Dora *et al*., 2022).

Barnes *et al*., (2015) suggested that PGE geochemistry can be used to identify the onset of sulphide saturation in magmatic rocks. Partial melting of the primitive mantle lead to the formation of either S-satuaration or S- undersaturated melts (Chen and Xie, 2008).The relationship between Cu and Pd has been identified as an useful indicator of degree of S-saturation of magmas (Chen and Xie, 2008). According to Said *et al*. (2011) Pt, Pd and Cu behave as incompatible elements during fractional crystallization of S-undersaturated magma. High MgO, low Ti, Al undepleted nature of the komatiites of the area exhibit high Cu/Pd ratios lower than that of primitive mantle thereby indicating removal of sulphides during magmatic evolution and S-undersaturation of the magma. The range of Ni/Cu (18.3-27.7) and Pd/Ir (12.67-42) suggest sulphide undersaturation condition for the rock of the present area.

Process Involved in the Formation of PGE

The komatiites of the present area have near chondritic Pt/Pd ratios (0.87-1.57), chondrite Pt/Pd=1.9. PGE data on komatiites (>3.3- ~2.6 Ga) have suggested that there is trend of increase in Pt and Pd abundance to younger ages in both Al-undepleted and Al-depleted komatiites (Puchtel *et al*., 2004). The Pt/Pd ratios of (0.87-1.57) may be due to HSE depletion during core formation followed by their addition during the long term event and mixing into Earth's deep mantle (Said *et al*., 2011).

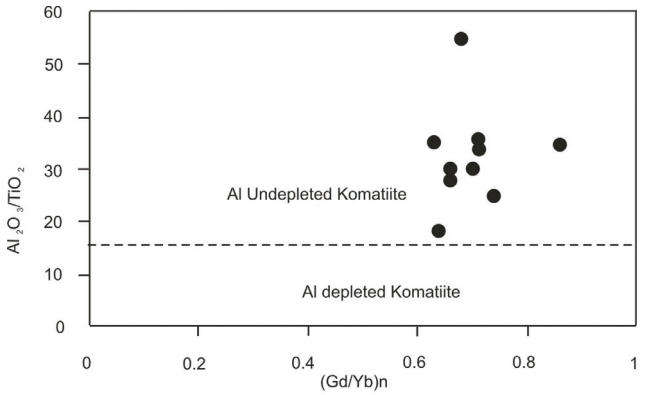

Fig. 6. Discrimination diagrams showing geochemical composition of Al-undepleted nature of the studied rock (Dostal and Mueller, 2004)

The rocks have Pd/Ir (12.67-66.1) and Pd/Pt (0.64-1.15) ratios higher than that of primitive mantle (Pd/Ir- 1.01; Pd/Pt- 0.53) and Chondrite (Pd/Ir-1.0; Pd/Pt-0.53). The Pt/Pd ratio of primitive mantle is 1.82 (McDonough and Sun, 1995) . Fractional crystallization of olivine and chromite during early stages of magmatic differentiation cause decoupling of Pt and Pd resulting into lowering of Pt/Pd ratios (Said *et al*., 2011) Pd and Ir concentration are controlled by sulphides and olivine respectively (Luguet *et al*., 2003). In the Pt/Pd ratio komatiites spread around the primitive mantle value of 1. Higher ratios of Pd/Ir with respect of Pt/Pd in the rock may be due to retaining of Ir and Pt within the refractory MSS (Monosulphide Solution) and Fe-Pt alloy whereas Pd would be easily mobilized and removed by Cu-S melt under relatively dry melting condition. Pentlandite dominated interstitial sulphides can show low Ir and high Pd/Ir ratios (Day *et al*., 2008). Wide range of Pd/Ir suggest that the PGE composition of these rocks are influenced by contamination from continental lithospheric mantle and PGE extraction during sulphide segregation. Maier (2005) have shown that Al-depleted komatiites of 3.5 Ga Barberton have lower PPGE content than Al-undepleted komatiites commonly found in 2.7 Ga greenstone belts and suggested that they formed by moderate degrees of partial melting that left some sulphide in the residue. The Pd/Ir ratios are low at low degree of partial melting and high at high degree of partial melting. When the partial melting reaches up to 20%, sulphides will be consumed which result in increase of Pd content (Said *et al*., 2011). Based on these observations a high degree partial melting accounts for the lower Pd and Pt contents and Pd/Ir ratios of the studied rock (Pd-3.5-18 ppb, Pt-5.04-18.72 ppb and Pd/Ir- 14.07-66.1).

Relative enrichment of PPGE in the studied rock with respect to IPGE reflect fractionation of the two groups. IPGEs like Pt, Ir, Ru show positive correlation with MgO suggesting fractionation of olivine in the parent magma. The studied rock fall in the fields of komatiites and mantle on Ni/Cu vs Pd/Ir discrimination diagram (Chen and Xie, 2008; Fig. 7a). Ni/Pd vs Cu/Ir plot (Barnes *et al*., 1985; Fig. 7b) shows an olivine fractionation trend for the komatiites of the area suggesting that PGE abundances in these

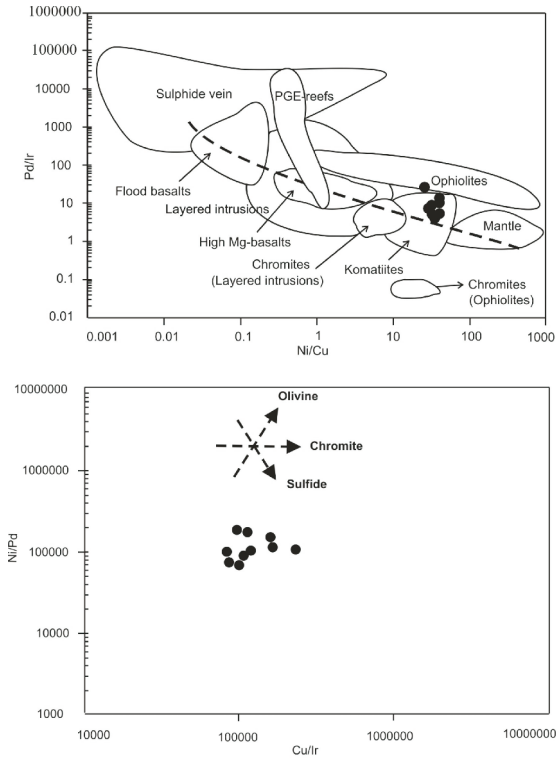

Fig. 7 a. Pd/Irv s Ni/Cu plot for the studied samples. (Fields *after* Chen and Xie, 2008), **b.** Cu/Ir vs Ni/Pd variation diagram in which the komatiites samples are following olivine fractionation trend (Fractionation trends *after* Barnes *et al.*, 1985).

rocks were dominantly controlled by olivine fractionation (Naldrett, 2010).

Primitive mantle normalized PGE patterns show (Fig.5c) distinct Pt enrichment which can be described as to early stage of fractional crystallization with >25% MgO. Variation in major elements with respect to Pd/Ir suggest the komatiites have consistently lower range of Pd/Ir with high MgO, low CaO and Al_2O_3 content. This observation indicates fractionation of IPGE into silicates phases during fractional cryastallisation. In the present study the S- undersatuarated komatiiites having PGE contents characterized by 3.5-18.0 ppb Pd and 5.23-18.72 ppb Pt are attributed to 73% partial melting at shallow depth and under anhydrous conditions. Enrichment of Pt, Rh and Pd relative to Iron primitive mantle normalized diagram can be ascribed to higher degree of partial melting of upper mantle. The PGE contents of most of the samples are in the global range of Al-undepleted komatiites with upto 15.1 ppb Pt, 20.9 ppb Pd, 8.99 ppb Ir, 6.35 ppb Ru and 27.7 ppb. Au (Guo *et al*., 2020). Except for Ir the studied rocks exhibit near similarities with global range. High Pt +Pd/Ir+Ru suggest that the rocks are formed by partial melting and crystal fractionation of olivine rich magma (Barnes *et al*.,1985).

Conclusions:

The ultramafic rocks are characterized by high MgO and chemically similar to komatiites and correspond to Al-undepleted Munro type komatiites suggesting presence of Meso to Neoarchaean segment in CGT. The Major, trace , REE and PGE composition of the rock suggest melting under anhydrous condition at shallow depth above the garnet stability field under S-undersaturated condition. Anhydrous melting associated with mantle plume activity gave rise to the komatiites. The rock shows contamination of lower crustal material during ascent and emplacement of magma. Crustal contamination played a significant role in PGE mineralization. They display primitive mantle-normalized patterns with positive Pt anomalies and is an example of silica hosted Pt-Au type mineralization. Magmatic Ni- Cu- PGE mineralization in the study area may be one of the prospective exploration targets.

Authors' Contributions

Jugnu Prasad: Investigation, Conceptualization, Formal analysis, Writing- original draft. **Deepak K. Bhattacharya:** Supervision, Reviewing and Editing.

Conflict of Interest

There is no conflict of Interest in this research publication.

Acknowledgements

The first author gratefully acknowledges the financial assistance from University Grants commission, New Delhi under the Post Doctoral Fellowship scheme for Women [No.F-15-1/2013-14/PDFWM-2013-14-OB-JHA-13159(SA-II)].

References

Arndt, N., Lesher, C.M. and Barnes, S.J. (2008). Komatiite. Cambridge University Press, New York, 467p.

Balaram, V. (2008) Recent advances in the determination of PGE in exploration studies- A review. Jour. Geol. Soc. India, v.72, pp. 661-677.

Balaram,V., Singh, S.P., Satyanarayanan, M. and Anjaiah, K.V. (2013). Platinum group elements geochemistry of ultramafic and associated rocks from Pindar in Mundwara Igneous Complex, Bundelkhand massif, Central India, Jour. Ear. Sys. Sci., v.122, pp. 79-91.

Barnes, S.J., Cruden, A.R., Arndt, N. and Saumur,B.(2015). The mineral system approach applied to magmatic Ni-Cu-PGE sulphide deposits. Ore Geol. Rev., doi:10.1016/j.oregeorev.2015.06.012.

Barnes, S.J., Naldrett, A. J. and Gorton, M.P. (1985). The origin of the fractionation of the platinum-group elements in terrestrial magmas. Chem. Geol.,v.53, pp.303-323.

Bhattacharya, D.K., Mukherjee, D.and Barla, V.C (2010). Komatiite within Chotanagpur Gneissic Complex at Semra, Palamau district Jharkhand. Petrological and geochemical fingerprints. Jour. Geol. Soc. India., v. 76, pp.589-606.

Bhowmik, S.K. (2019). The current status of orogenesis in the central Indian tectonic zone: A view from its southern margin. Geol. Jour., v. 54, pp.2912-2934., doi :10.1002/gi. 3456.

Blichert-Toft, J., Arndt, T.N., Wilson, A. and Coetzee (2015).Hf and Nd isotope systematic of early Archean komatiites from surface sampling and ICDP drilling in Barberton Greenstone Belt. South Africa Americ. Mineralog., v.100, pp. 2396-2411.

Chen, G. and Xie, B.(2008). Platinum-group elemental geochemistry of mafic and ultramafic rocks from the Xigazeophiolite, southern Tibet.

Jour. Asian Earth Sci., v.32, pp.406-422.

Condie, K.C. and Kroner, A.(2013). The building blocks of continental crust: evidence for a major change in the tectonic setting of continental growth at the end of the Archean. Gond. Res.,v.23, pp.394-402.

Day, J.M.D., Pearson, D.G. and Hulbert, L. (2008). Rhenium-osmium isotope and platinum group element constrsints on the origin and evolution of the 1.27 Ga Muskox intrusion. Jour. Petrol., v.49, pp.1255-1295.

Dostal, J. and Muellar, W.U. (2004). Komatiite Geochemistry: Developments in Precambrian Geology, Elsevier, Amsterdam, v.12, pp. 290-298.

Dora, M.L., Meshram, T., Baswani, S.R., Malviya, V.P., Mahapatro, S.N., Dash, J.K., Meshram, R.R., Verma, S.K., Wankhade, S.H., Mohanty, M., Pati, P. and Randive, K. (2022). The Paleo-Mesoarchaean Gondpipri Mafic-Ultramafic Intrusions, Western Bastar Archaean Craton, Central India: Insights from Bulk-Rock Geochemistry and Sm-Nd and S Isotope Studies on the Formation of Ni-Cu-PGE Mineralisation. Eco. Geol., https://doi.org/10.5382/ econgeo.4947.

Fiorentini, M.L., Barnes, S.J., Maier, W.D., Burnharm, O.M. and Heggie, G. (2011). Global variability in the platinum-group element contents of komatiites. Jour. Petrol., v.52, pp.83-112.

Ghose, N.C. and Chatterjee, N. (2008).Petrology,tectonic setting and source of dykes and related magmatic bodies in the Chotanagpur Gneissic Complex,eastern India. *In*: Srivastava, R.K., Sivaji, C.H. and Chalapathi, Rao. N.V. (*Eds.*) Indian Dykes. Narosa Publishing House, New Delhi, pp. 471-493.

Govingdaraju, K. (1994). Compilation of working values and sample description for 383. Geostandards Newsletter, v.18, Spec. issue, pp.1a-158.

Guo, F.F., Svetov, S., Maier, W.D., Hanski, E., Yang, S. H. and Rybnikova, Z. (2020). Geochemistry of komatiites and basalts in Archean greenstone belts of Russian Karelia with emphasis on platinum-group elements. Minerali. Deposit., v.55, pp.971-970.

Jenson, L.S. (1976). A new method of classifying alkali volcanic rocks. Ontario Division Mineral, Misc. Paper no. 66, 22p.

Krishna, A.K., Murthy, N.N. and Goril, P.K. (2007) Multielement analysis by wavelength dispersive X-ray Fluorescence spectrometry. Atom. Spectroscop., v. 28(6), pp. 212-214.

Lesher, C.M. and Barnes, S.J. (2009). Komatiite associated Ni-Cu-(PGE) deposits. In: Li, C. PGE Deposits: Genetic Models and Exploration. Geological Publishing House of China, pp.27-101.

Luguet, A., Lorand, J.P. andSeyler, M. (2003). Sulfide petro;ogy and highly siderophile element geochemistry of abyssal peridotites: a coupled study of samples from the kane Fracture Zone (45° W:23° 20'N, mark area, Atlantic Ocean). Geochim. Cosmochim. Acta, v.67, pp.1553-1570.

Maier,W.D.(2005). Platinum-group element (PGE) deposits and occurrences Mineralisation styles, genetic concepts, and exploration criteria. Jour. Afric. Earth Sci., v.41, pp.165-191.

Manikyamba, C. and Saha, A. (2014). PGE geochemistry of komatiites from Neoarchean Sigegudda greenstone terrane western Dharwar Craton, India. In: Krishnamurthy, P., Vidyadharan, K.T. and Sawkar, R.H. (Eds.). Proceedings of the Workshop on Magmatic Ore Deposits. Geol. Soc. India. Spec. Publ., v. 2, pp.162-174.

Maya, J.M., Rajneesh Bhutani, R., Balakrishnan, S. and Sandhya, S.R. (2017). Petrogenesis of 3.15 Ga old Banasandra komatiites from the Dhawar craton, India: Implications for early mantle heterogeneity. Geosci. Front., v.8(3), pp.467-481.

McDonough, W.F. and Sun, S.S. (1995). The composition of the earth. Chem. Geol., v.120, pp. 223-253.

Mondal, S.K. (2011). Platinum Group Element (PGE) Geochemistry to understand the Chemical Evolution of the Earth's Mantle. Jour. Geol. Soc. India, v.77, pp. 295-302.

Mukherjee, S., Dey, A., Sanyal, S. and Sengupta, P. (2019). Proterozoin crustal evolution of the Chotanagpur granite gneissic complex, Jharkhand-Bihar-West Bengal, India: Current status and future prospect. Tectonics and structural Geology: Indian context (*Ed.* S. Mukherjee), Cham: Springer Geology International Publishing AG, pp.7-54.

Naldrett, A. (2010). From the mantle to bank: the life of a Ni-Cu-(PGE) deposit. South African Jour. Geol., v.113, pp.1-32.

Negi, P.,Saikia, A., Ahmad, M., Upadhyay, D. and Akhtar, S. (2022) . Nature and origin of anorthosite enclaves within Proterozoic granite of Chotanagpur Granite Gneiss Complex of Eastern India. Front. Earth Sci. 10:952554., doi: 10.3389/feart.2022.952554.

Patel, R., Shankar, R., Sharma, D.S. and Panda, A. (2021). Geochemistry and Petrogenesis of tholeiitic dykes from the Chotanagpur Gneissic Complex, eastern India. Jour. Earth Syst. Sci., https://doi.org/10.1007/s12040-021-01646-7.

Prasad, J., Bhattacharya, D.K. and Barla, V.C. (2012). Geochemical Character and Tectonic Significance of Amphibolites from south of Daltonganj, Palamau district, Jharkhand. Gomd. Geol. Mag., v. 27(1), pp. 55-66.

Prasad, J. and Bhattacharya, D.K. (2013). Platinum group of elements in Semra komatiite, Palamau District, Jharkhand: A preliminary observation. Jour. Geol. Soc. India, v.82, pp.607-612.

Puchtel, I.S., Humayun,M.,Campbell, A.J.,Sproule, R.A. and Lesher, C.M. (2004). Platinum group element geochemistry of komatiites from the alexo and Pyke Hill areas,Ontario, Canada. Geochim. Cosmochim. Acta, v.68,pp.1361-1383.

Rao, N.V.C., Srivastava, R.K., Sinha, A.K. and Ravikant,V. (2014).Petrogenesis of Kerguelen mantle plume-linked Early Cretaceous ultrapotassic intrusive rocks from the Gondwana sedimentary basins, Damodar Valley, Eastern India. Earth Sci. Rev., v.136, pp.96-120.

Rekha, S., Upadhyay, D., Bhattacharya, A., Kooijman, E., Goon, S., Mahato, S. and Pant, N.C. (2011).Lithostructural and Chronological constraints for tectonic restoration of Proterozoic accretion in the Eastern Indian Precambrian Shield. Precamb. Res., v. 187(3-4), pp. 313-333.

Said, N., Kerrich, R., Maier, W.D. and McCuaig, C. (2011). Behaviour of Ni-PGE-Au-Cu in mafic-ultramafic volcanic suites of the 2.7 Ga Kambalda Sequence, Kalgoorlie Terrane, Yilgarn Craton. Geochim. Cosmochim. Acta, v.75, pp. 2882-2910.

Saha, A., Manikyaamba, C., Santose, M., Ganguly, S. and Khelen, A. C. (2015). Platinum Group Elements (PGE) geochemistry of komatiites and boninites from Dharwar Craton, India: Implications for mantle melting processes. Jour. Asian Earth Sci., v. 105, pp. 300-319.

Sanyal, S. and Sengupta, P. (2012). Metamorphic evolution of the Chotanagpur Granite Gneiss Complex of the East Indian Shield: Current status. *In*: Paleoproterozoic of India Geological Society (*Eds.* Mazumder, R. and Saha, D.), Geol. Soc. London Spec. Publ., v.365,pp.117-145.

Sun, S.S. and McDonough, W.F. (1989). Chemical and isotopic systematic of oceanic basalts: Implications for mantle composition and process. In: Magmatism in the ocean basins (Eds. A.D. Saunders and M.J. Norry (London: Geol Soc Spec Publ), v. 42, pp. 313-345.

Tushipokla and Jayananda, M.(2013). Geochemical constraints on komatiite volcanism from Sargur Group Nagamangala greenstonebelt, Western Dharwar Craton, Southern India: Implications for Mesoarchean mantle evolution and continental growth. Geosci. Front., v. 4, pp. 321-340.

Viljoen, M.J., Viljoen, R.P. and Pearton, T.N.(1982). The nature and distribution of Archean komatiite volcanic in South Africa. *In*: Arndt, N.T.; Nisbet, E.G (*Eds.*) Komatiites Allen and Unwin London, pp.53-79.

Zhou, M.F., Robinson, Pt. Su, B.X., Gao, J.F., Li, J. W. Yang, J.S., and Malps, J. (2014). Compositions of chromite associated minerals and parental magmas of podiform chromite deposits the role of slab contamination of asthenospheric melts in suprasubduction zone environments. Gond. Res., v.26, pp. 262-283.